

# Bayesian Analysis and Constraints on Kinematic Models from Union SNIa

A.C.C. Guimarães, J.V. Cunha and J.A.S. Lima

Departamento de Astronomia, Universidade de São Paulo,  
Rua do Matão 1226, CEP 05508-090 São Paulo SP, Brazil

E-mail: aguimaraes@astro.iag.usp.br, cunhajv@astro.iag.usp.br,  
limajas@astro.iag.usp.br

**Abstract.** The kinematic expansion history of the universe is investigated by using the 307 supernovae type Ia from the Union Compilation set. Three simple model parameterizations for the deceleration parameter (constant, linear and abrupt transition) and two different models that are explicitly parametrized by the cosmic jerk parameter (constant and variable) are considered. Likelihood and Bayesian analyses are employed to find best fit parameters and compare models among themselves and with the flat  $\Lambda$ CDM model. Analytical expressions and estimates for the deceleration and cosmic jerk parameters today ( $q_0$  and  $j_0$ ) and for the transition redshift ( $z_t$ ) between a past phase of cosmic deceleration to a current phase of acceleration are given. All models characterize an accelerated expansion for the universe today and largely indicate that it was decelerating in the past, having a transition redshift around 0.5. The cosmic jerk is not strongly constrained by the present supernovae data. For the most realistic kinematic models the  $1\sigma$  confidence limits imply the following ranges of values:  $q_0 \in [-0.96, -0.46]$ ,  $j_0 \in [-3.2, -0.3]$  and  $z_t \in [0.36, 0.84]$ , which are compatible with the  $\Lambda$ CDM predictions,  $q_0 = -0.57 \pm 0.04$ ,  $j_0 = -1$  and  $z_t = 0.71 \pm 0.08$ . We find that even very simple kinematic models are equally good to describe the data compared to the concordance  $\Lambda$ CDM model, and that the current observations are not powerful enough to discriminate among all of them.

*Keywords:* supernova type Ia - standard candles, dark energy experiments, dark energy theory

## 1. Introduction

The extension of the Hubble diagram to larger distances by using observations from supernovae type Ia (SNIa) as standard candles, allowed the history of cosmic expansion to be probed with deeper detail. Independent measurements by various groups indicated that the current expansion is in fact speeding up and not slowing down, as believed for many decades [1, 2, 3, 4]. In other words, in virtue of some unknown mechanism, the expansion of the Universe underwent a “dynamic phase transition” whose main effect is to change the sign of the universal deceleration parameter  $q(z)$ .

The physical explanation for such a transition is one of the greatest challenges for cosmology today. Inside the General Relativity paradigm, it requires the presence of a cosmological constant in the cosmic equations, or to postulate the existence of an exotic fluid with negative pressure (in addition to dark matter), usually called dark energy [5, 6, 7, 8, 9], or even a gravitationally-induced cold dark matter creation [10, 11, 12]. Another possibility is to change the theory describing the gravitational interaction as happens, for instance, in the framework of the so-called F(R) modified gravity theories [13, 14, 15, 16, 17]. In both cases, the space parameter associated with the cosmic expansion is too degenerate, and, as such, it is not possible, based on the current data, to decide which mechanism or dark energy component is operating in the cosmic dynamics [18].

Another very distinct firsthand approach to access the history of the cosmic expansion without the use of quantities coming from the dynamic description has also been proposed in the literature [19]. This route is very interesting because it depends neither on the validity of any particular metric theory of gravity nor on the matter-energy content of the observed Universe. It is closely related to the weaker assumption that space-time is homogeneous and isotropic, so that the FRW metric is still valid, as are the kinematic equations for redshift/scale factor. Some call it cosmography [20, 22] or cosmokinetics [23], others use the term Friedmannless cosmology [24, 25], but, in what follows, we refer to it simply as a kinematic approach since it holds true regardless of the underlying cosmic dynamics [3, 26, 27, 28, 29, 30].

Few years ago, Elgarøy & Multamäki [25] investigated constraints on some kinematic models by employing a Bayesian marginal likelihood analysis based on the Gold Supernova sample data of Riess et al. [3] and the Supernova Legacy Survey (SNLS) of Astier et al. [4]. In their analysis of the flat case, three different parameterizations for an accelerating  $q(z)$  model were examined, namely: constant, linear, and abrupt transition, respectively,  $M_0$ ,  $M_1$  and  $M_2$  in their nomenclature. It was also argued that any expansion of the jerk parameter (the third order contribution in the expansion for kinematic luminosity distance in terms of the redshift  $z$ ) could be seen as requiring more parameters, or cosmic fluids in the dynamic approach, than expanding the deceleration parameter. In addition, it was also observed that the flat  $\Lambda$ CDM and the Einstein-de Sitter model have constant jerk parameter  $j_0 = -1$ , and, therefore, it cannot be used for discriminating such cosmologies. Accordingly, their analysis was restricted to the deceleration parameter.

In this work we go one step further by examining the case for the jerk parameter (constant and variable). One basic reason is that the bi-dimensional space parameter  $(q_0, j_0)$  can naturally discriminate the flat  $\Lambda$ CDM and Einstein-de Sitter models because they have different predictions for  $q_0$ . Actually, it is not necessary to expand  $j(z)$ , thereby introducing many parameters in order to have a larger class of models, since this happens even for constant jerk. Probably, and more importantly, it is not clear a priori if the Bayesian evidence prefers the cosmic concordance model when a more general constant jerk parameter is considered. Potentially, a constant jerk parameter provide

us with the simplest approach to search for departures from the cosmic concordance model. For completeness, in our analysis we also consider all the flat models discussed by Elgarøy & Multamäki [25], however, we also examine the predictions of two different approaches including constant and variable jerk parameters. In addition, and differently from previous works, the present Bayesian analysis is based on the larger Union Compilation SNIa data recently published by Kowalski et al. [31].

## 2. Kinematic Models

Assuming that the universe is homogeneous and isotropic above some scale, the Friedmann-Robertson-Walker (FRW) metric provides a good description of the geometry of the universe ( $c = 1$ )

$$ds^2 = dt^2 - a^2(t) \left[ \frac{dr^2}{1 - kr^2} + r^2 d\Omega \right], \quad (1)$$

where  $k$  is the space curvature that we will assume hereafter to be null, since the current emerging consensus is that the universe is flat or very close to flat [18]. The function  $a(t)$  is the scale factor, which contains the complete history of the cosmic expansion and can be parameterized by the redshift,  $a = (1 + z)^{-1}$  ( $a_0 = 1$ ).

The rate of expansion and the acceleration are represented by the Hubble and deceleration parameters, respectively

$$H \equiv \frac{\dot{a}}{a}, \quad (2)$$

and

$$q \equiv -\frac{1}{H^2} \frac{\ddot{a}}{a} = \frac{1}{2}(1 + z) \frac{[H(z)^2]'}{H(z)^2} - 1. \quad (3)$$

Similarly, the jerk parameter is defined as

$$j \equiv -\frac{1}{H^3} \frac{\dot{\ddot{a}}}{a} = -\left[ \frac{1}{2}(1 + z)^2 \frac{[H(z)^2]''}{H(z)^2} - (1 + z) \frac{[H(z)^2]'}{H(z)^2} + 1 \right]. \quad (4)$$

The basic aim here is to examine some simple kinematic models for the cosmic expansion based on specific parameterizations for  $q(z)$  in (3) and a constant jerk parameter.

The first and simplest model,  $M_0$ , is given by a constant deceleration parameter,  $q(z) = q_0$ . The second model,  $M_1$ , is a linear expansion of the deceleration parameter  $q(z) = q_0 + q_1 z$  (first used by [3]). Model  $M_2$  (introduced by [19]) depicts two phases of constant deceleration parameter, separated by an abrupt transition redshift,  $q(z) = q_0$  for  $z \leq z_t$  and  $q(z) = q_1$  for  $z > z_t$ . The fourth model,  $M_3$ , is a constant jerk parametrization,  $j(z) = j_0$  (examined for the first time by [3]). As one may show, the cosmic jerk is related with the deceleration parameter by the differential equation

$$j = -\left[ q + 2q^2 + (1 + z) \frac{dq}{dz} \right]. \quad (5)$$

It should be stressed that kinematic models with constant jerk parameter are also very attractive because the historically important dynamical EdS cosmology and, with more generality, the flat  $\Lambda$ CDM scenario are particular cases for which  $j(z) = j_0 = -1$ .

On the other hand, it is widely known that if one wishes to describe the recent cosmic expansion, then the current values of the parameters given by (2), (3) and (4) lead to the late time cosmic expansion [32, 20]

$$a(t) = 1 + H_0(t - t_0) - \frac{1}{2}q_0H_0^2(t - t_0)^2 - \frac{1}{3!}j_0H_0^3(t - t_0)^3 + \mathcal{O}[(t - t_0)^4], \quad (6)$$

from which the luminosity distance can be expanded, yielding an extended version of the Hubble law [33]

$$d_L(z) = \frac{c}{H_0} \left[ z + \frac{1}{2}(1 - q_0)z^2 - \frac{1}{6}(1 - q_0 - 3q_0^2 - j_0)z^3 \right] + \mathcal{O}(z^4), \quad (7)$$

where the highest order term depends on fourth order and higher derivatives of the scale factor. A shortcoming of this series is that for supernovae at  $z > 1$  the  $\mathcal{O}(z^4)$  terms may be large in principle, *i.e.*, there is a convergence problem [34]. Nevertheless, most of the known supernovae are at  $z < 1$  and a truncation of (7) always can be seen as a polynomial fit. So we define our last model,  $M_4$ , as the third order truncation of (7), which also has as free parameters  $q_0$  and  $j_0$ . However, differently from  $M_3$ , this model has variable jerk parameter (see A.19).

In the Appendix, one may find the basic analytical expressions for all models investigated in the present work.

### 3. Sample and Statistical Analysis

In the statistical analysis below we consider the most complete supernovae data set currently available, namely, the Union supernova sample as compiled by Kowalski et al. [31]. The Union SNIa compilation is a new data set at low and intermediate nearby-Hubble-flow redshifts whose analysis procedures permit to work with several heterogeneous supernova samples. It includes 13 independent sets, and, after selection cuts, the robust compilation obtained is composed by 307 SNIa events distributed over the redshift interval  $0.015 \leq z \leq 1.62$ .

In figure 1 we show the behaviour and dispersion of the data in the reduced Hubble-Sandage diagram. The curves correspond to the models considered in this work, as indicated in the legend. For the sake of comparison, we also show the present cosmic concordance model.

The distance moduli  $\mu$  is defined as the difference between the apparent ( $m$ ) and absolute ( $M$ ) magnitudes, so that the observed and theoretical values are respectively

$$\mu_{obs,i} = m_{obs,i} - M, \quad (8)$$

and

$$\mu_{th}(z_i) = m_{th}(z_i) - M = 5 \log_{10} d_L(z_i, p) + \mu_0, \quad (9)$$

where  $\mu_0 = 25 - 5 \log_{10} H_0$ , and  $d_L$  is the luminosity distance

$$d_L(z, p) = (1 + z) \int_0^z \frac{du}{H(u)}, \quad (10)$$

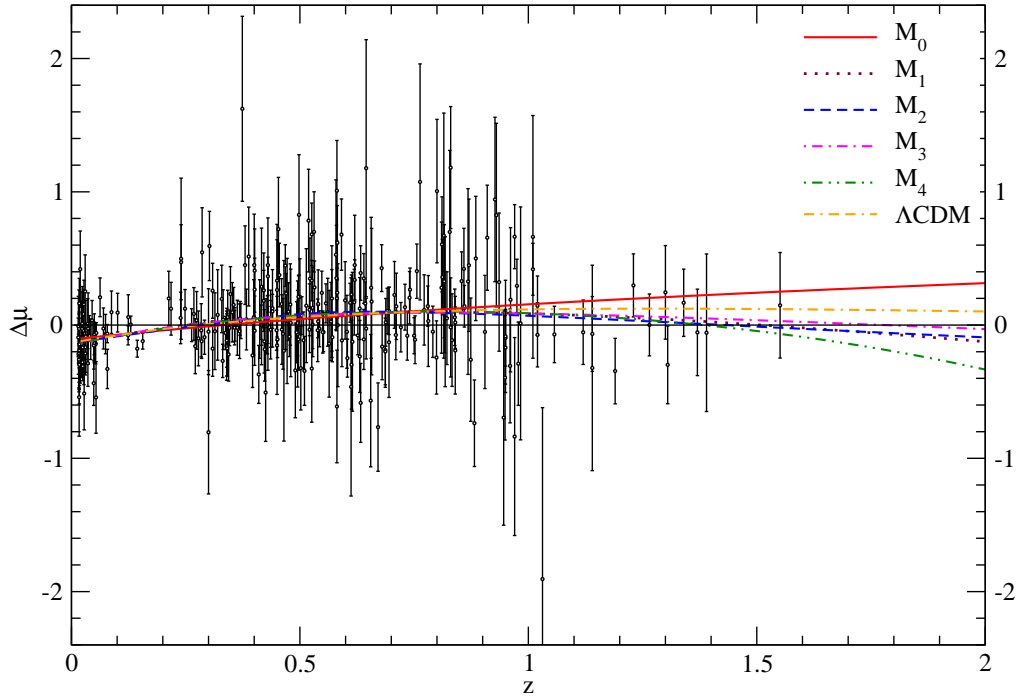


**Figure 1.** Kinematic model predictions for SNe Ia data. Residual magnitude versus redshift is displayed for 307 SNe type Ia from SCP union compilation. The predictions of five kinematic models ( $M_0 - M_4$ ) are displayed relative to an eternally coasting model, for which  $H(z) = H_0(1+z)$  and  $q(z) \equiv 0$ . For comparison, the cosmic concordance model has also been included. Note that for  $z > 1.5$ , the model with  $j$  is a free parameter constant ( $M_3$ ) is the closest one to  $\Lambda$ CDM.

which carries the model parameter dependencies represented by  $p$ .

The likelihood analysis is based on the calculation of

$$\chi^2(p, \mu_0) \equiv \sum_{SNIa} \frac{[\mu_{obs,i} - \mu_{th}(z_i)]^2}{\sigma_i^2} \quad (11)$$

$$= \sum_{SNIa} \frac{[\mu_{obs,i} - 5 \log_{10} d_L(z_i, p) - \mu_0]^2}{\sigma_i^2}. \quad (12)$$

We analytically marginalize over the nuisance parameter  $\mu_0$  [27],

$$\tilde{\chi}^2(p) = -2 \ln \int_{-\infty}^{+\infty} \exp \left[ -\frac{1}{2} \chi^2(p, \mu_0) \right] d\mu_0, \quad (13)$$

to obtain

$$\tilde{\chi}^2 = a - \frac{b^2}{c} + \ln \left( \frac{c}{2\pi} \right), \quad (14)$$

where

$$a = \sum_{SNIa} \frac{[5 \log_{10} d_l(z_i, p) - \mu_{obs,i}]^2}{\sigma_i^2}, \quad (15)$$

$$b = \sum_{SNIa} \frac{5 \log_{10} d_l(z_i, p) - \mu_{obs,i}}{\sigma_i^2}, \quad (16)$$

$$c = \sum_{\text{SNIa}} \frac{1}{\sigma_i^2}. \quad (17)$$

The nuisance parameter value that minimizes (12) is  $\mu_0 = b/c$ . The expression  $\chi^2(p, b/c) = a - (b^2/c)$  is sometimes used instead of (14) to perform the likelihood analysis. Both are equivalent if the prior for  $\mu_0$  is flat, as is implied in (13), and the errors  $\sigma_i$  are model independent, what also is the case here. For the SNIa sample used we find  $\tilde{\chi}^2(p) - \chi^2(p, b/c) = \ln(c/2\pi) \approx 7.2$ .

To determine the best fit parameters for each model, we minimize  $\tilde{\chi}^2(p)$ , what is equivalent to maximizing the likelihood

$$\mathcal{L}(p) \propto e^{-\tilde{\chi}^2(p)/2}. \quad (18)$$

The Bayesian evidence can then be calculated as

$$E \equiv \int \mathcal{L}(p) P(p) dp = \frac{1}{V_P} \int_{V_P} \mathcal{L}(p) dp, \quad (19)$$

where  $P(p)$  is the prior probability distribution for the parameters, which we adopt to be flat, and  $V_P$  is the volume in the parameter space defined by the prior intervals. We chose conservative prior intervals (see table 1) based on physical considerations and “prior” information, *i.e.* previous results obtained with older and smaller SNIa samples [22, 25, 27, 34]. The prior boundaries are chosen to be large enough so most of the likelihood is retained in the integration (19), but not too large to do not excessively penalize the Bayesian evidence through  $V_P$ . For all the models considered here, except for  $M_2$ , as will be discussed in the next section, the  $3\sigma$  boundaries in the likelihood are well inside the prior volume, so the Bayesian evidence decreases linearly with  $V_P$ .

We are able to compare models by calculating the Bayes factor between any two models  $M_i$  and  $M_j$ , which we define as

$$B_{ij} = \frac{E(M_j)}{E(M_i)}. \quad (20)$$

Some authors [35, 36] offer qualitative interpretations of the Bayes factor value (Jeffreys scale) that say how one model is favoured over the other, given the data and priors. Note that under our convention of the Bayes factor, if  $E(M_j) > E(M_i)$  than  $\ln B_{ij}$  is positive.

#### 4. Results and Discussion

In figure 2 we show the likelihood results for the kinematic models considered and also for the  $\Lambda$ CDM model for comparison. The horizontal axis depicts the deceleration parameter today in the same scale for all models to facilitate the comparison among models. At the panels for  $\Lambda$ CDM and  $M_0$  the full likelihood is plotted as a function of  $q_0$  — we use that  $q_0 = \frac{3}{2}\Omega_m - 1$  for  $\Lambda$ CDM, see (A.22) — since these models have only one free parameter. For the other models it is presented the confidence contours in two dimensional parameter spaces (we marginalize over  $z_t$  for model  $M_2$  that has three

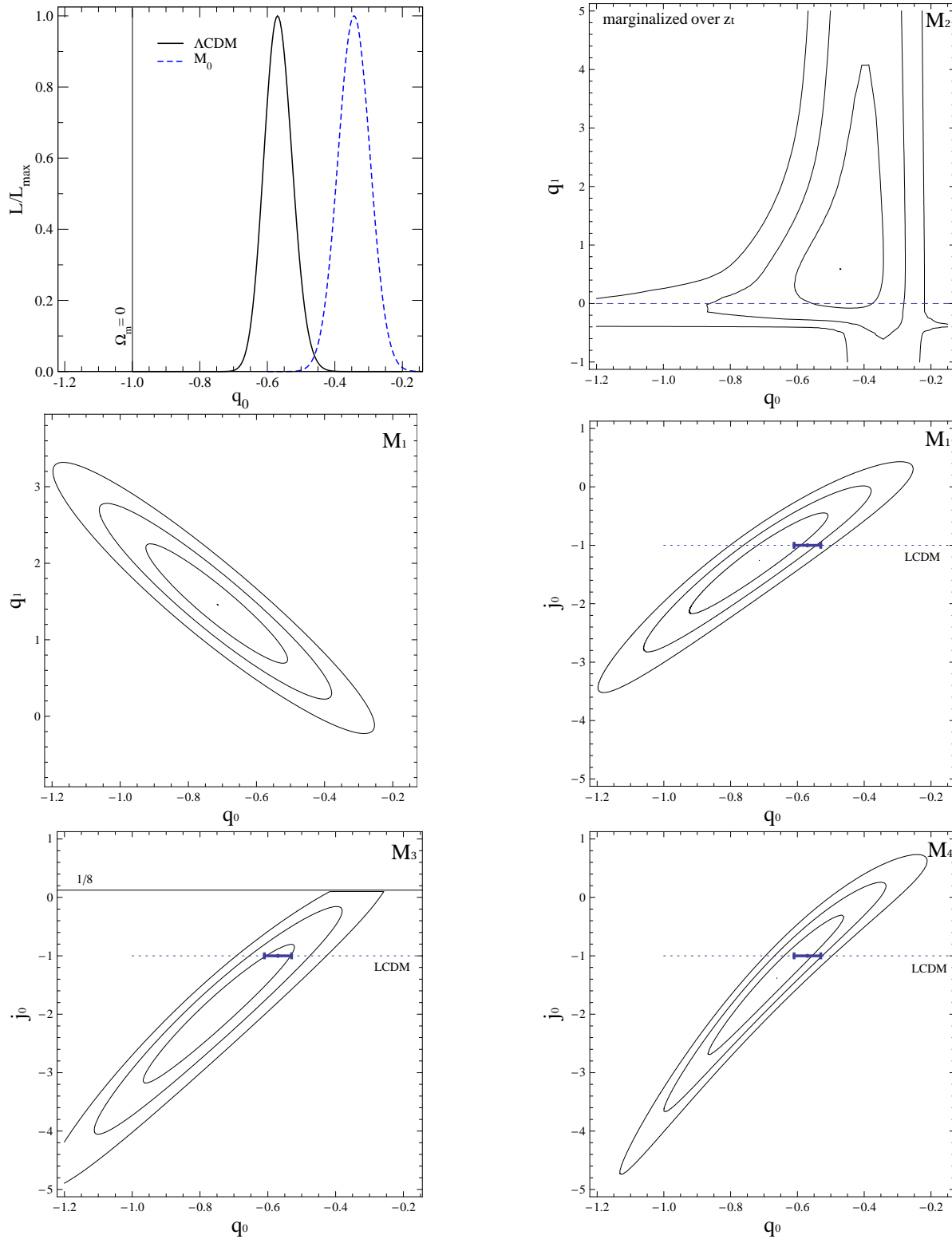


**Figure 2.** Likelihood results for all studied models (labels on the top of each panel). The top left panel is for models with one free parameter ( $\Lambda$ CDM and  $M_0$ ). The remaining panels show the likelihood contours in the parameter space of each model, delimiting the  $1\sigma$ ,  $2\sigma$  and  $3\sigma$  confidence regions. Model  $M_1$  is also shown in the  $(q_0, j_0)$  parameter space. The dotted line in three of the panels depicts the image of  $\Lambda$ CDM models in the  $(q_0, j_0)$  parameter space representation and the error bar corresponds to the  $1\sigma$  region for the best  $\Lambda$ CDM fit. The solid straight lines on the panels for  $\Lambda$ CDM and  $M_3$  depict the allowed regions in parameter space for these models.

Model	$q_0$	$j_0$	$z_t$	$V_P$	$\tilde{\chi}_{red}^2$	$\ln B_{0i}$
$\Lambda$ CDM	$-0.57 \pm 0.04$	$-1$	$0.71^{+0.08}_{-0.07}$	1	1.043	3.6
$M_0 : q = q_0$	$-0.34 \pm 0.05$	$0.11 \pm 0.02$	no transition	2	1.065	0
$M_1 : q = q_0 + q_1 z$	$-0.71 \pm 0.21$	$-1.3^{+0.8}_{-0.9}$	$0.49^{+0.27}_{-0.09}$	10	1.040	3.5
$M_2 : q = \begin{cases} q_0, z \leq z_t \\ q_1, z > z_t \end{cases}$	$-0.49^{+0.13}_{-0.26}$	$0.01^{+0.09}_{-0.38}$	$0.46^{+0.40}_{-0.28}$	18	1.043	2.1
$M_3 : j = j_0$	$-0.74 \pm 0.22$	$-1.9^{+1.1}_{-1.3}$	$0.48^{+0.36}_{-0.11}$	10	1.041	3.3
$M_4 : d_L(z)$ expansion	$-0.66 \pm 0.20$	$-1.4^{+1.1}_{-1.3}$	$0.52^{+0.21}_{-0.08}$	12	1.040	3.2

**Table 1.** Models, maximum likelihood estimates of the universal kinematic parameters ( $q_0, j_0, z_t$ ) and  $1\sigma$  projected errors, prior volume, goodness of fit and Bayes factor in relation to  $M_0$ . All models are in a flat universe,  $V_P$  is the prior volume; priors are  $q_0 \in [-2, 0]$  for all kinematic models,  $q_1 \in [-1, 4]$  for  $M_1$ ,  $q_1 \in [-1, 5]$  and  $z_t \in [0, 1.5]$  for  $M_2$ ,  $j_0 \in [-5, 1/8]$  for  $M_3$ ,  $j_0 \in [-5, 1]$  for  $M_4$ , and  $\Omega_m \in [0, 1]$  for  $\Lambda$ CDM. The relations between the particular model parameters and the universal kinematic parameters are given in the Appendix.

degrees of freedom). The equations for  $M_3$  — see (A.15) in the Appendix — indicate that the maximum physical value for  $j_0$  in this model is  $1/8$ , so we limit the graph to this region.

Table 1 contains the maximum likelihood values and  $1\sigma$  projected errors for the deceleration and jerk parameter today and for the transition redshift. Note that some of these parameters are the best fit values for free parameters of the models and others are derived quantities from them. See the Appendix for the expressions. Table 1 also presents the parameter space volume of the priors for each model; the goodness of fit as quantified by  $\tilde{\chi}_{red}^2 \equiv \tilde{\chi}_{min}^2 / (N - n_p)$ , where  $N$  is the number of data points and  $n_p$  is the number of free parameters in each model; and the Bayes factor in relation to model  $M_0$ .

The deceleration today is significantly negative in all models, but its exact value and uncertainty are model-dependent. The likelihoods for models with just one degree of freedom ( $M_0$  and  $\Lambda$ CDM) are very peaked in  $q_0$  (see top left panel of figure 2), yielding a more precise determination of this parameter, and consequentially also of  $j_0$ , than in the other models (see table 1). For the models of constant acceleration today ( $M_0$  and  $M_2$ ) the current values of the cosmic jerk are in disagreement with the values found for the remaining models, which are compatible among themselves and with the  $\Lambda$ CDM prediction. The values of the transition redshift determined in all kinematic models are close to  $z_t \sim 0.5$ , and are compatible in  $1\sigma$  with the higher value obtained in the  $\Lambda$ CDM model.

Our likelihood contours for model  $M_1$  at figure 2 are qualitatively similar, but with tighter constraints, to what was obtained in previous works [3, 25]. We also represent the  $M_1$  model in the parameter space of the deceleration and jerk today, making use of (A.6).



The panel for  $M_2$  shows a qualitatively similar plot to the last panel of figure 2 of Shapiro & Turner [22]. The  $z_t$  marginalized likelihood contours for  $M_2$  at  $2\sigma$  and  $3\sigma$  confidence levels show that the data do not constrain strongly the deceleration parameter for redshifts above the transition. The parameter  $q_1$  can assume very large positive values and also negative values. In this last case, represented by the points below the dashed line on the  $M_2$  panel of figure 2,  $z_t$  is a transition redshift between two accelerated phases. Points above the dashed line represent situations in which there is a transition from a decelerated phase at high  $z$  to an accelerated phase at low  $z$ . We also tested a larger upper prior boundary for  $q_1$ , but even for  $q_1 = 10$  the  $2\sigma$  likelihood contour is open (in this case  $\ln B_{02} = 1.6$ ).

Models  $M_3$  and  $M_4$  (bottom panels at figure 2), and  $M_1$  as well, have roughly similar likelihood contours in the  $(q_0, j_0)$  plane due to the relation (5), implying similar determinations of  $q_0$  and  $j_0$ , similar goodness of fit and Bayesian evidences. These likelihood contours also show that the best fit  $\Lambda$ CDM model, represented by a  $1\sigma$  error bar over the dotted line with  $j_0 = -1$ , is compatible at  $1\sigma$  confidence level with  $M_1$ ,  $M_3$  and  $M_4$ . Similar result was obtained by Rapetti et al. [27] using a joint analysis of the Gold [3] and SNLS [4] SNIa samples and X-ray cluster gas mass fraction measurements. When considering separately the SNIa sets, those authors found  $j_0 = -2.8_{-1.2}^{+1.1}$  for the Gold set and  $j_0 = -1.3_{-1.4}^{+1.2}$  for the SNLS set. We also examined the case where just supernovae with  $z < 1$  (289 events) were fitted by model  $M_4$  and the results do not differ considerably from the ones for the full sample (307 events). In fact, the goodness of fit is worst for the subsample with  $z < 1$ ,  $\tilde{\chi}_{red}^2 = 1.057$ .

All models, except  $M_0$ , have similar goodness of fit, as quantified by  $\tilde{\chi}_{red}^2$ . In fact, if we observe the best fit curves at figure 1, it is very difficult to judge which one best describes the data. The Bayes factor segregates  $M_0$  from the other models, but only weakly disfavours  $M_2$  over the remaining models, mainly because of the penalizing effect of the larger prior volume of  $M_2$  (due to it having three free parameters) in relation to the other models. The basic result is that the Bayes factor is unable to significantly distinguish models  $M_1$ ,  $M_3$ ,  $M_4$  and  $\Lambda$ CDM. This is a somewhat different result from what was found by Elgarøy & Multamäki [25] when examining separately the Gold [3] and SNLS [4] SNIa sets. There the authors obtained a clear ranking of the models based on the Bayes factor (see their table 5), even though these rankings were different for the two SNIa samples.

It is worth to note that the behaviour for the evolution of the deceleration parameter is very distinct among the models considered here. The simplest kinematic models,  $M_0$ ,  $M_1$  and  $M_2$ , have self-evident  $q(z)$ , but  $M_3$  has a more subtle, and interesting acceleration history. For this model  $q(z)$  — given by (A.12) — has a qualitatively similar behaviour to that of  $\Lambda$ CDM (A.22), namely, asymptotic constant values in the past and future with a smooth transition around  $z_t$ . For  $\Lambda$ CDM the asymptotic limits are fixed,  $q(z \rightarrow \infty) = 0.5$  and  $q(z \rightarrow -1) = -1$ , but for  $M_3$  they will depend on  $q_0$  and  $j_0$ . In the specific case of our best fit values for  $M_3$ ,  $q(z \rightarrow \infty) \sim 0.76$  and  $q(z \rightarrow -1) \sim -1.3$ . There is no deceleration in the future in this model, and therefore,

no new phase transition. For  $M_4$  the extrapolation of  $q(z)$  is not expected to be valid far from the redshift range for which it was adjusted, and, in fact, (A.18) presents nonphysical behaviour in the extremes past and future. None of our models are able to hint at any slowing down of the cosmic acceleration today or in the future, such as suggested recently [37] in the context of an extended SNIa sample.

## 5. Summary and Conclusions

Bellow we summarize our main accomplishments and conclusions.

1. We perform, for the first time, a kinematic analysis of the 307 SNIa compiled in the Union set [31]. This approach, also called Friedmanless, allows us to analyse the cosmic expansion just having to assume the homogeneity and isotropy of the universe, and not having to make any assumption about the underlying gravitational theory and energy components of the universe.

2. We employ several kinematic models that were used by different groups with various SNIa samples before. Using a unified framework and a single data set, we are able to compare the kinematic models directly. We calculate for each model the goodness of fit (as measured by  $\chi_{red}^2$ ) and the Bayes factor. Even very simplistic kinematic models can give an equivalent description of the cosmic expansion to the one provided by the currently favoured concordance  $\Lambda$ CDM model. More to the point, current data is not powerful enough to clearly discriminate among some of these simple models. This is a distinct conclusion from what Elgarøy & Multamäki [25] obtained using separately the SNLS and Gold samples for a particular class of the models studied here, and who found conflicting results from the two samples. Nevertheless, some kinematic models ( $M_1$ ,  $M_3$  and  $M_4$ ) were shown to be superior, or more realistic, than kinematic models with constant deceleration ( $M_0$  and  $M_2$ ).

3. We give, for all kinematic models studied, the expressions and estimates for a minimal set of parameters that characterizes the recent history of the cosmic expansion:  $q_0$  (deceleration today),  $j_0$  (cosmic jerk today) and  $z_t$  (transition redshift from a decelerated to an accelerated phase).

4. Independently of models, the universe is in a phase of accelerated expansion, however the value of the deceleration parameter today is model-dependent. For the most realistic kinematic models ( $M_1$ ,  $M_3$  and  $M_4$ ),  $q_0$  is in the  $1\sigma$  range  $[-0.96, -0.46]$ .

5. There is evidence that the deceleration parameter was higher and positive in the past, implying a transition from a decelerated phase to an accelerated one. The transition redshift between these two phases is found to be around 0.5 in all kinematic models, being in the  $1\sigma$  range  $[0.36, 0.84]$  for the the most realistic kinematic models. That is compatible in  $1\sigma$  with the higher value predicted by  $\Lambda$ CDM.

6. The value of the cosmic jerk today can be used as a measure of a possible deviation from a  $\Lambda$ CDM model, which exactly predicts  $j_0 = -1$  by definition. For the models with constant deceleration today ( $M_0$  and  $M_2$ ) the value for  $j_0$  is significantly higher than for  $\Lambda$ CDM, but these models no longer have a strong cosmological appeal.

The remaining kinematic models ( $M_1$ ,  $M_3$  and  $M_4$ ) have a slight preference for  $j_0 < -1$ , being in the  $1\sigma$  range  $[-3.2, -0.3]$ . But at the current confidence level yielded by the data there is no significant departure from the  $\Lambda$ CDM prediction. We note that the constant jerk model is an interesting parameterization of the cosmic expansion because, among other reasons, it contains popular models as  $\Lambda$ CDM and EdS.

Finally, taking into account the discussion in the previous section, about the behaviour of the deceleration parameter in the context of jerk models, it could be interesting to extend the present work by allowing additional contributions from a snap parameter (dependent on the fourth order derivative of the scale factor). Either in a simplified model,  $s(z) = \text{constant}$ , as well as in an expansion of the luminosity distance. Hopefully, this may help us to have some indication about a possible dynamic transition in the future, with the universe entering in a new decelerating phase [38]. Some work along these lines will be presented in a forthcoming communication.

## Acknowledgements

ACCG is supported by FAPESP under grant 07/54915-9. JVC is supported by FAPESP under grant 05/02809-5 and partially also by CNPq under grant 477190/2008-1. JASL is partially supported by CNPq and FAPESP under grants 304792/2003-9 and 04/13668-0, respectively.

## Appendix A. Kinematic Expressions

In this appendix we show the analytical expressions for the basic quantities in all models investigated in the present work.

### $M_0$

$$H(z) = H_0(1+z)^{1+q_0} \quad (\text{A.1})$$

$$q(z) = q_0 \quad (\text{A.2})$$

$$j(z) = -(q_0 + 2q_0^2) \quad (\text{A.3})$$

### $M_1$

$$H(z) = H_0(1+z)^{1+q_0-q_1} e^{q_1 z} \quad (\text{A.4})$$

$$q(z) = q_0 + q_1 z \quad (\text{A.5})$$

$$j(z) = -[q(z) + q^2(z) + (1+z)q_1] \quad (\text{A.6})$$

$$z_t = -q_0/q_1 \quad (\text{A.7})$$

### $M_2$

$$H(z) = \begin{cases} H_0(1+z)^{1+q_0}, & z \leq z_t \\ H_0(1+z_t)^{q_0-q_1}(1+z)^{1+q_1}, & z > z_t \end{cases} \quad (\text{A.8})$$

$$q(z) = \begin{cases} q_0, & z \leq z_t \\ q_1, & z > z_t \end{cases} \quad (\text{A.9})$$

$$j(z) = \begin{cases} -(q_0 + 2q_0^2), & z \leq z_t \\ -(q_1 + 2q_1^2), & z > z_t \end{cases} \quad (\text{A.10})$$

### $\mathbf{M}_3$

$$H(z) = H_0 [c_1(1+z)^{\alpha_1} + c_2(1+z)^{\alpha_2}]^{\frac{1}{2}} \quad (\text{A.11})$$

$$q(z) = \frac{c_1(1+z)^{\alpha_1}(\frac{\alpha_1}{2} - 1) + c_2(1+z)^{\alpha_2}(\frac{\alpha_2}{2} - 1)}{c_1(1+z)^{\alpha_1} + c_2(1+z)^{\alpha_2}} \quad (\text{A.12})$$

$$j(z) = j_0 \quad (\text{A.13})$$

$$z_t = \left[ -\frac{c_2 \alpha_2 - 2}{c_1 \alpha_1 - 2} \right]^{\frac{1}{\alpha_1 - \alpha_2}} - 1 \quad (\text{A.14})$$

where

$$\alpha_{1,2} = \frac{3}{2} \pm \sqrt{\frac{9}{4} - 2(1+j_0)} \quad (\text{A.15})$$

$$c_1 = \frac{2(1+q_0) - \alpha_2}{\alpha_1 - \alpha_2} \quad \text{and} \quad c_2 = 1 - c_1 \quad (\text{A.16})$$

From (A.15) we see that  $j_0 < \frac{1}{8}$ .

$\mathbf{M}_4$  – defined by the expanded luminosity distance (7),  $d_L(z) = \frac{c}{H_0} (z + Az^2 + Bz^3)$ , where  $A = (1 - q_0)/2$  and  $B = -(1 - q_0 - 3q_0^2 - j_0)/6$ .

$$H(z) = H_0 \left[ \frac{(1+z)^2}{1 + 2Az + (A + 3B)z^2 + 2Bz^3} \right] \quad (\text{A.17})$$

$$q(z) = \frac{1 - 2A - 2(A + 3B)z - (A + 9B)z^2 - 2Bz^3}{1 + 2Az + (A + 3B)z^2 + 2Bz^3} \quad (\text{A.18})$$

$$j(z) = -[q + 2q^2 + (1+z)q'] \quad (\text{A.19})$$

$$z_t : \text{the real root of } 1 - 2A - 2(A + 3B)z_t - (A + 9B)z_t^2 - 2Bz_t^3 = 0 \quad (\text{A.20})$$

### $\Lambda$ CDM, $\Omega_m + \Omega_\Lambda = 1$

$$H(z) = H_0 [\Omega_m(1+z)^3 + (1 - \Omega_m)]^{\frac{1}{2}} \quad (\text{A.21})$$

$$q(z) = [(1+z)^3 - 2(1/\Omega_m - 1)] / [2(1+z)^3 + 2(1/\Omega_m - 1)] \quad (\text{A.22})$$

$$j(z) = -1 \quad (\text{A.23})$$

$$z_t = [2(\Omega_m^{-1} - 1)]^{\frac{1}{3}} - 1 \quad (\text{A.24})$$

Note that the expressions for  $\Lambda$ CDM can be easily obtained from (A.11-A.14), putting  $j_0 = -1$  into (A.15). If we do similarly for  $M_0$ , putting  $j_0 = -(q_0 + 2q_0^2)$  into (A.15), we recover the right expressions for  $H(z)$  and  $q(z)$ , and, curiously,  $z_t = -1$ . This just illustrates that all models with a particular constant jerk are particular cases of  $M_3$ .

## References

- [1] Riess A G *et al.* 1998 *Astron. J.* **116** 1009 [astro-ph/9805201]
- [2] Perlmutter S *et al.* 1999 *Astrophys. J.* **517** 565 [astro-ph/98121330]
- [3] Riess A G *et al.* 2004 *Astrophys. J.* **607** 665 [astro-ph/0402512]
- [4] Astier P *et al.* 2006 *Astron. & Astrophys.* **447** 31 [astro-ph/0510447]
- [5] Peebles P J E and Ratra B 2003 *Rev. Mod. Phys.* **75** 559 [astro-ph/0207347]
- [6] Padmanabhan T 2003 *Phys. Rept.* **380** 235 [hep-th/0212290]
- [7] Lima J A S 2004 *Braz. Journ. Phys.* **34** 194 [astro-ph/0402109]
- [8] Copeland E J M and Tsujikawa S 2006 *Int. J. Mod. Phys.* **D15** 1753 [hep-th/0603057]
- [9] Frieman J A, Turner M S and Huterer D 2008 *Ann. Rev. Astron. & Astrophys.* **46** 385
- [10] Lima J A S, Germano A S M. and Abramo L R W 1996 *Phys. Rev. D* **53** 4287
- [11] Lima J A S, Silva F E and Santos R C 2008 *Class. Quant. Grav.* **25** 205006
- [12] Steigman G, Santos R C and Lima J A S 2009 *JCAP* **6** 33
- [13] Barrow J D and Cotsakis S 1988 *Phys. Lett. B* **214** 515
- [14] Li B and Barrow J D 2007 *Phys. Rev. D* **75** 084010 [gr-qc/0701111]
- [15] Amarguoui M, Elgarøy Ø, Mota D F and Multamäki T 2006 [astro-ph/0510519] *Astron. Astrophys.* **454** 707
- [16] Fairbairn M and Rydbeck S 2007 *JCAP* **0712** 005[astro-ph/0701900]
- [17] Carvalho F C, Santos E M, Alcaniz J S and Santos J 2008 *JCAP* **9** 8 [arXiv:0804.2878]
- [18] Komatsu E *et al.* (WMAP Collaboration) 2009 *Astrophys. J. Suppl.* **180** 330 [arXiv:0803.0547]
- [19] Turner M S and Riess A G 2002 *Astrophys. J.* **569** 18 [astro-ph/0106051]
- [20] Visser M 2004 *Class. Quant. Grav.* **21** 2603 [gr-qc/0309109]
- [21] Visser M 2005 *General Relativity and Gravitation* **37** 1541 [gr-qc/0411131]
- [22] Shapiro C and Turner M S 2006 *Astrophys. J.* **649** 563 [astro-ph/0512586]
- [23] Blandford R D, Amin M, Baltz E A, Mandel K and Marshall P J 2005 *Observing Dark Energy*, 339, 27 [astro-ph/0408279]
- [24] Elgarøy Ø and Multamäki T 2005 *Mon. Not. Roy. Astron. Soc.* **356** 475 [astro-ph/0404402]
- [25] Elgarøy Ø and Multamäki T 2006 *JCAP* **9** 2 [astro-ph/0603053]
- [26] Virey J-M *et al.* 2005 *Phys. Rev. D* **72** R061302
- [27] Rapetti D, Allen S W, Amin M A. and Blandford R D 2007 *MNRAS* **375** 1510 [astro-ph/0605683]
- [28] Daly R A *et al.* 2008 *Astrophys. J.* **677** 1
- [29] Cunha J V and Lima J A S 2008 *Mon. Not. R. Astron. Soc.* **390** 210 [arXiv:0805.1261]
- [30] Cunha J V 2009 *Phys. Rev. D* **79** 047301 [arXiv:0811.2379]
- [31] Kowalski M *et al.* 2008 *Astrophys. J.* **686** 749 [arXiv:0804.4142]
- [32] Weinberg S 1972 *Cosmology and Gravitation*(John Wiley Sons, New York)
- [33] Chiba T, Nakamura T 1998, *Progress of Theoretical Physics* **100** 1077
- [34] Cattoën C, Visser M 2007, arXiv:gr-qc/0703122
- [35] Jeffreys H 1961 *Theory of Probability* (Oxford: Clarendon Press)
- [36] Trotta R 2007 *Mon. Not. Roy. Astron. Soc.* **378** 72 [astro-ph/0504022]
- [37] Shafieloo A, Sahni V, and Starobinsky A A 2009 arXiv:0903.5141
- [38] Carvalho F C, Alcaniz J S, Lima J A S, Silva R 2006 *Phys. Rev. Lett.* **97** 081301 [astro-ph/0608439]